2017 IEEE-RAS 17th International Conference on
Humanoid Robotics (Humanoids)
Birmingham, UK, November 15-17, 2017

# Towards a Better Understanding of Human Sprinting Motions With and Without Prostheses

Anna Lena Kleesattel[1], Wolfgang Potthast[2] and Katja Mombaur[1]

***Abstract*— Amputee sprinting motions are of high interest due to the remarkable performances of individual athletes and the resulting question what the share of their running-specific prostheses is. The goal of our study was to compare twelve able-bodied and amputee sprinting motions which were synthesized by combinations of ten optimality criteria. We created rigid multi-body system models with 13 degrees of freedom in the sagittal plane for both an able-bodied and an amputee sprinter. The joints are powered by torque actuators, except for the prosthetic joint which is equipped with a passive linear spring-damper system. The sprinting motions are the solutions of an optimal control problem with periodicity constraints and objective functions which combine different optimality criteria. For both athletes, we found realistic human-like sprinting motions. The analysis of the motions suggested that the amputee athlete applies less active joint torque in the hip and knee of his affected leg compared to the able-bodied athlete.**

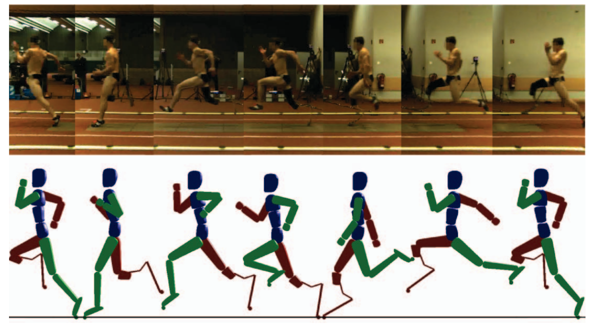

Fig. 1: Comparison of a high-speed video (recorded at German Sport University Cologne) and an optimized solution

## I. INTRODUCTION

The significantly increasing performances of amputee sprinters and long-jumpers over the last years repeatedly raise concerns regarding their running-specific prostheses. Those devices are made up of carbon fiber and thus have spring-like properties which might be advantageous in comparison to a human ankle. The fact that the discussion about advantage or disadvantage is still not settled emphasizes the complexity of human sprinting motions. Even without prosthetic devices, the whole body needs to coordinate. Hence, a better understanding is of considerable interest in many areas of research such as biomechanics, robotics and computer graphics. Amputee motions are useful to understand how humans interact with technical aids and how such technology alters the way of moving. This more profound understanding of human movement in connection with technical aids is relevant to the humanoids community as well.

The basic kinematics and dynamics of human sprinting without and also with prostheses is already quite well understood [9], [16]. A huge amount of biomechanical studies is based on the analysis of recorded kinematic motion capture data, often in combination with force platform or sensor insole measurements for information about the dynamics [8], [21]. Other researchers focus on the analysis of publicly available video recordings to investigate basic characteristics of sprinting such as step length or step frequency [10], [14]. The existing sprinting models range from simple inverted pendulum and spring-mass models [4], [7] to very precise and complex ones including muscle dynamics [15], [19]. A concurring outcome in the comparison of able-bodied and double transtibial amputee athletes is that they have completely different movement patterns and actuation strategies [3], [22]. However, those comparisons are mainly done for double transtibial amputee athletes.

Despite this already available knowledge about human sprinting, specifying optimality criteria, i.e. characteristic quantities which are minimized or maximized in sprinting, is a rather difficult task. It seems quite obvious that the athletes aim to maximize their speed, hence to accelerate as fast as possible and keep the reached velocity over the whole race. A common assumption is that the sprinting velocity in $100\,\mathrm{m}$ sprint is the product of step frequency and step length [1], [10]. Therefore, two possible criteria are maximizing the step frequency and maximizing the step length. Salo and colleagues [18] reported that the reliance on step frequency and step length is highly individual in elite sprinters, i.e. some mainly maximize either step frequency or step length and some use combinations of both. Weyand and co-workers [21] found similar mean aerial times for fast and slow runners due to comparable vertical impulses which are accomplished by different combinations of force and ground contact times though. They concluded that the fast speeds are achieved by applying greater ground forces during short contact phases.

In our research, we apply mathematical modeling and optimal control methods for both motion analysis and motion synthesis. In a previous paper, we have shown first results of the dynamics reconstruction of an able-bodied and an amputee sprinter for the purpose of further analyzing practical motion capture data [11]. In this paper, we focus

[1]Anna Lena Kleesattel and Katja Mombaur are with the Optimization, Robotics & Biomechanics (ORB) research group, Institute of Computer Engineering (ZITI), Heidelberg University, 69120 Heidelberg, Germany {annalena.kleesattel, katja.mombaur }@ziti.uni-heidelberg.de

[2]Wolfgang Potthast is with the Institute of Biomechanics and Orthopaedics, German Sport University, 50933 Köln, Germany Potthast@dshs-koeln.de

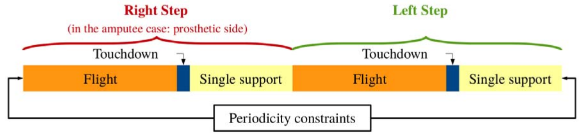


Fig. 2: Phases of human sprinting which we used for the multi-phase optimal control problem formulation

on the generation of sprinting motions using an optimal control approach with appropriate optimality criteria. Such an approach has been successfully used before for synthesizing human walking [5] and human sprinting [17], [20]. In [17], Mombaur compared sprinting of able-bodied and double transtibial amputee athletes which was synthesized by minimizing the joint torques and found remarkably lower joint torques in the double amputee case.

We want to extend those investigations to unilateral transtibial amputee sprinting and more optimality criteria. Thus, we aimed to answer the following questions:

1) Which optimality criteria are adopted in human sprinting with and without prostheses?
2) Are the joint torques significantly lower in the optimized solution of the unilateral transtibial amputee?

In this paper, we first present the rigid multi-body systems that we established for an able-bodied and a unilateral transtibial amputee sprinter. We then describe the optimal control problem formulation for the computation of optimal sprinting motions and how it is solved numerically. Finally, we discuss the different optimality criteria that we used to generate able-bodied and amputee sprinting motions. We compare those motions with reference motion capture data as well as with each other to answer the above defined research questions.

## II. MODELING HUMAN SPRINTING MOTIONS WITH AND WITHOUT PROSTHESES

We model the sprinting motions as a sequence of alternating flight and single-leg contact phases. In this paper, we consider two full steps where the start and end point are marked by the toe-off of the left foot (see Fig. 2).

Each of those phases is described by its own set of ordinary differential (ODE) or differential-algebraic equations (DAE). Within the flight phase, both feet are off the ground. The motion of the human model is then governed by

$$\boldsymbol{M}(\boldsymbol{q})\,\ddot{\boldsymbol{q}} + N(\boldsymbol{q},\dot{\boldsymbol{q}}) = \boldsymbol{\tau}\,, \tag{1}$$

where $\boldsymbol{M}(\boldsymbol{q})$ is the inertia matrix and $N(\boldsymbol{q},\dot{\boldsymbol{q}})$ is the vector of non-linear effects including Coriolis and gravitational forces. The generalized positions, velocities, accelerations and forces acting on the rigid multi-body system are denoted by $\boldsymbol{q}, \dot{\boldsymbol{q}}, \ddot{\boldsymbol{q}}$ and $\boldsymbol{\tau}$.

The contact phase is characterized by the point-like contact of one foot with the ground which causes external constraints on the rigid multi-body model. Such a model with $m$ external constraints is described by the following DAE of index 3:

$$\boldsymbol{M}(\boldsymbol{q})\,\ddot{\boldsymbol{q}} + \boldsymbol{N}(\boldsymbol{q},\dot{\boldsymbol{q}}) = \boldsymbol{\tau} + \boldsymbol{G}(\boldsymbol{q})^T\,\boldsymbol{\lambda}\,, \tag{2a}$$

$$\boldsymbol{g}(\boldsymbol{q}) = 0\,. \tag{2b}$$

The matrix $\boldsymbol{G}(\boldsymbol{q}) = \frac{\partial}{\partial \boldsymbol{q}}\boldsymbol{g}(\boldsymbol{q})$ is the so-called contact Jacobian and $\boldsymbol{\lambda}$ are the contact forces. By differentiating the constraint equation (2b) twice, we can rewrite (2) as a linear system of the unknowns $\ddot{\boldsymbol{q}}, \boldsymbol{\lambda}$:

$$\begin{bmatrix} \boldsymbol{M}(\boldsymbol{q}) & \boldsymbol{G}(\boldsymbol{q})^T \\ \boldsymbol{G}(\boldsymbol{q}) & \boldsymbol{0} \end{bmatrix} \begin{bmatrix} \ddot{\boldsymbol{q}} \\ -\boldsymbol{\lambda} \end{bmatrix} = \begin{bmatrix} -\boldsymbol{N}(\boldsymbol{q},\dot{\boldsymbol{q}}) + \boldsymbol{\tau} \\ \gamma(\boldsymbol{q},\dot{\boldsymbol{q}}) \end{bmatrix}\,. \tag{3}$$

The term $\gamma(\boldsymbol{q},\dot{\boldsymbol{q}})$ is called contact Hessian. The system is always solvable if the constraints in $\boldsymbol{g}(\boldsymbol{q})$ are independent. To ensure equivalence of (2) and (3), we need to impose constraints at the beginning of the contact phase which make sure that the invariants of the constraints are fulfilled.

As elite sprinters use a forefoot-running technique, we use a point-like contact with the ball of the foot. We further assume the contact to be rigid and non-sliding. At phase transitions, discontinuities in the state variables can occur. The timing of the phase transitions is not prescribed but depends on the position variables of the human. It is formulated by switching functions

$$s(\boldsymbol{q}(t_s)\,, \dot{\boldsymbol{q}}(t_s)\,, p) = 0\,, \tag{4}$$

which define the touchdown and lift-off events as follows: Touchdown occurs when the $z$-position of the contact point equals zero and the lift-off event is prescribed by the vertical ground reaction force becoming zero.

The touchdown of the foot is treated as an instantaneous collision which we assume to be completely inelastic since there is hardly any compliance in spiked running shoes. The discontinuous change in the generalized velocities can be computed by

$$\begin{bmatrix} \boldsymbol{M}(\boldsymbol{q}) & \boldsymbol{G}(\boldsymbol{q})^T \\ \boldsymbol{G}(\boldsymbol{q}) & \boldsymbol{0} \end{bmatrix} \begin{bmatrix} \dot{\boldsymbol{q}}^+ \\ -\Lambda \end{bmatrix} = \begin{bmatrix} \boldsymbol{M}(\boldsymbol{q})\,\dot{\boldsymbol{q}}^- \\ \boldsymbol{0} \end{bmatrix}\,, \tag{5}$$

where $\dot{\boldsymbol{q}}^{+/-}$ are the velocities before and after the collision respectively and $\Lambda$ is the contact impulse. The upper row states the conservation of momentum of the system and the lower row the velocity after the collision.

We do not require symmetry between the right and the left step, but we do consider periodic motions, i.e. periodicity constraints ensure that all position variables (except the one associated with the forward direction), all velocity variables and all torque variables are identical at the start and the end of a pair of steps (compare Fig. 2).

As models of such complexity cannot be derived on paper, we use the rigid body dynamics library RBDL [6] to generate the equations of motion.

To analyze the sprinting motions, we use two models, one of a unilateral transtibial amputee athlete and - for reference purpose - one of an able-bodied sprinter (see Fig. 3). Both are established as rigid multi-body system models consisting of 14 segments (thighs, shanks, feet/prosthetic device, lower,

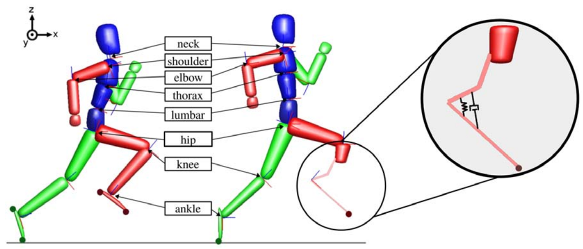


Fig. 3: Models of an able-bodied athlete and an amputee athlete with a running-specific prosthesis

middle & upper trunk, head, upper & lower arms) with 16 degrees of freedom (DOF) in the sagittal plane. Three global DOF describe the two-dimensional movement of the floating base. The remaining 13 internal DOF account for the rotations of the joints around the y-axis. The restriction to a 2D model is justified by the fact that short-distance sprinting involves mainly forward motions. At this stage of our research, we do not include a muscle model, but assume the action of all muscles at a joint to be summarized by an artificial joint torque actuator. The prosthetic device which is modeled by rigid components with a rotational joint, is not actuated since the athletics regulations only allow for passive devices. Instead we include a linear spring-damper system to account for the spring-like properties of the running-specific prosthesis. The prosthesis is coupled to the residual shank by a fixed joint as we do not consider movements between the residual limb and the prosthesis. The spring and damping constants are fixed to the values which we found in reconstructing the dynamics of motion capture data [11].

We use an extrapolation of the de Leva data [13] to the measured heights and weights (amputee athlete: $1.83\,\mathrm{m}$, $76.0\,\mathrm{kg}$; able-bodied athlete: $1.80\,\mathrm{m}$, $75.4\,\mathrm{kg}$). The model of the prosthetic device was created with respect to data measured at the German Sport University Cologne.

## III. OPTIMAL CONTROL PROBLEM FORMULATION

In our optimal control problem, we solve for the optimal state trajectories $\boldsymbol{x}(t) = [\boldsymbol{q}(t), \dot{\boldsymbol{q}}(t), \boldsymbol{\tau}(t)]^T$, control trajectories $\boldsymbol{u}(t) = \dot{\boldsymbol{\tau}}(t)$, free parameters $\boldsymbol{p}$ and phase durations $t_1, \dots, t_4$. The optimal control problem can be stated in the following general form:

$$\min_{\boldsymbol{x}(\cdot), \boldsymbol{u}(\cdot), \boldsymbol{p}, \boldsymbol{t}} \quad \phi(\boldsymbol{x}(t), \boldsymbol{u}(t), \boldsymbol{p}) \tag{6a}$$

subject to:

$$\dot{\boldsymbol{x}}(t) = \boldsymbol{f}_i(\boldsymbol{x}(t), \boldsymbol{u}(t), \boldsymbol{p}) , \tag{6b}$$
$$\boldsymbol{x}(t_i^+) = \boldsymbol{c}_i(\boldsymbol{x}(t_i^-)) , \tag{6c}$$
$$0 \le \boldsymbol{g}_i(\boldsymbol{x}(t), \boldsymbol{u}(t), \boldsymbol{p}) , \tag{6d}$$
$$0 \le \boldsymbol{r}(\boldsymbol{x}(\hat{t}_1), \dots, \boldsymbol{x}(\hat{t}_k), \boldsymbol{p}) , \tag{6e}$$

with $t \in [t_{i-1}, t_i], i = 1, \dots, 4$ and $\hat{t}_i$ are the times at the shooting nodes. Equation (6a) is the objective function in which the optimality criteria are formalized. We describe the objective function in III-A in more detail.

The differential states $\boldsymbol{x}(t)$ are the generalized positions $\boldsymbol{q}(t)$, the generalized velocities $\dot{\boldsymbol{q}}(t)$ and the generalized forces $\boldsymbol{\tau}(t)$. As controls, we use the derivatives of the joint torques $\boldsymbol{u}(t) = \dot{\boldsymbol{\tau}}(t)$. The velocity at the end point, the spring and the damping constant are fixed parameters of the problem where the latter are only present in the amputee case.

Equations (6b) and (6c) are placeholders for the dynamics of the system. They are evaluated as described in II. The phase durations are not prescribed. Instead, phase transitions are defined by the lift-off and touchdown events.

The path constraints (6d) consist of upper and lower bounds for the differential state and control variables. The bounds are obtained from the dynamics reconstruction solution [11] by computing the minimum and maximum values of the optimized trajectories and adding an offset. The offset is needed as we only considered one particular motion for each athlete.

The non-linear point constraints (6e) impose additional conditions such as kinematic limitations at touchdown and toe-off and proper ground reaction forces. The vertical ground reaction forces should be positive during ground contact such that the model is not pulled by the ground. For the horizontal ones we impose a friction cone constraint.

### A. Objective Functions

To synthesize sprinting motions, we have formulated ten optimality criteria based on previous experience in optimization of human movement, a literature review and expert guesses which we assume to cover the most relevant criteria. Four of them are evaluated at the end of a phase and thus have to be written as objective functions of Mayer type. The remaining six objective functions are of Lagrange type, i.e. they are evaluated during the respective phase. Combining all optimality criteria, the objective function reads

$$\begin{aligned}\phi(\boldsymbol{x}(t), \boldsymbol{u}(u), \boldsymbol{p}) &= \sum_{j=1}^{j=4} \left(\gamma_j \phi_{M_j}(t_f, \boldsymbol{x}(t_f), \boldsymbol{p})\right) \\ &+ \sum_{i=1}^{N} \int_{t_{i-1}}^{t_i} \left( \sum_{j=5}^{10} \gamma_j \phi_{L_j}(t, \boldsymbol{x}(t), \boldsymbol{u}(t), \boldsymbol{p}) \right) \mathrm{d}t \,.\end{aligned} \tag{7}$$

The weighting factors $\gamma_j, j = 1, \dots, 10$ are used to scale quantities of different magnitude to comparable size (e.g. joint torques and angular momentum values), to get different combinations of the basic criteria and to account for importance of the respective criterion in sprinting motions. The basic optimality criteria are:

*a) Minimize Relative Contact Time:* The objective function that minimizes the duration of the contact phase $t_{contact}$ with respect to the total time $T$ is stated as a Mayer term:

$$\phi_{M_1}(t_f, \boldsymbol{x}(t_f), \boldsymbol{p}) = \frac{1}{T} t_{contact} \,. \tag{8}$$

*b) Maximize Step Frequency:* The step frequency is the inverse of the time $t_{step}$ needed to perform one step. As it is evaluated at the end of the contact phase, we state it as

TABLE I: Weighting coefficients for the formulation of objective functions from basic optimality criteria

| | Name | $\gamma_1$ | $\gamma_2$ | $\gamma_3$ | $\gamma_4$ | $\gamma_5$ | $\gamma_6$ | $\gamma_7$ | $\gamma_8$ | $\gamma_9$ | $\gamma_{10}$ |
|---|---|---|---|---|---|---|---|---|---|---|---|
| $\phi_1$ | *Min. Relative Contact Time* | 1 | 0 | 0 | 0 | 0 | $10^{-8}$ | 0 | 0 | 0 | 0 |
| $\phi_2$ | *Max. Step Frequency* | 0 | 1 | 0 | 0 | 0 | $10^{-8}$ | 0 | 0 | 0 | 0 |
| $\phi_3$ | *Max. Vertical Ground Impact* | 0 | 0 | 1 | 0 | 0 | $10^{-7}$ | 0 | 0 | 0 | 0 |
| $\phi_4$ | *Max. Stride Length* | 0 | 0 | 0 | 1 | 0 | $10^{-9}$ | 0 | 0 | 0 | 0 |
| $\phi_5$ | *Min. Torques Squared* | 0 | 0 | 0 | 0 | 1 | $10^{-4}$ | 0 | 0 | 0 | 0 |
| $\phi_6$ | *Min. Torque Derivatives Squared* | 0 | 0 | 0 | 0 | 0 | 1 | 0 | 0 | 0 | 0 |
| $\phi_7$ | *Head Stabilization* | 0 | 0 | 0 | 0 | 0 | 1 | $10^9$ | 0 | 0 | 0 |
| $\phi_8$ | *Min. Angular Momentum over CoM* | 0 | 0 | 0 | 0 | 0 | $10^{-8}$ | 0 | 1 | 0 | 0 |
| $\phi_9$ | *Max. Vertical Ground Reaction Forces* | 0 | 0 | 0 | 0 | 0 | $10^{-6}$ | 0 | 0 | 1 | 0 |
| $\phi_{10}$ | *Max. Horizontal Ground Reaction Forces* | 0 | 0 | 0 | 0 | 0 | $5 \times 10^{-7}$ | 0 | 0 | 0 | 1 |
| $\phi_{11}$ | *Multiple Objective Criteria I* | 0 | 1 | 0 | 1.5 | 0 | $10^{-8}$ | 10 | 0 | 0 | 0 |
| $\phi_{12}$ | *Multiple Objective Criteria II* | 0 | 0 | 0 | 1 | 0 | $10^{-8}$ | 10 | 0 | 0 | 0 |

an objective function of Mayer type:

$$\phi_{M_2}(t_f, \boldsymbol{x}(t_f), \boldsymbol{p}) = -\frac{1}{t_{step}} . \tag{9}$$

*c) Maximize Vertical Ground Impact:* The ground impact whose vertical component is denoted by $j_{vertical}$ indicates how hard the athlete pushes the ground at touchdown:

$$\phi_{M_3}(t_f, \boldsymbol{x}(t_f), \boldsymbol{p}) = -j^2_{vertical} . \tag{10}$$

This criterion formalizes a behavior which is observed in amputee sprinting.

*d) Maximize Stride Length:* The stride length is defined as the distance between the hallux point of the left foot at the beginning and the end of the two-step cycle. In the optimal control problem, it is incorporated as a parameter $p_d$:

$$\phi_{M_4}(t_f, \boldsymbol{x}(t_f), \boldsymbol{p}) = -p_d . \tag{11}$$

*e) Minimize Torques Squared:* This objective function which minimizes the squared torques, is a measure of the effort it takes to perform sprinting at the given velocity.

$$\phi_{L_5}(t, \boldsymbol{x}(t), \boldsymbol{u}(t), \boldsymbol{p}) = \|\boldsymbol{\tau}(t)\|_2^2 . \tag{12}$$

*f) Minimize Torque Derivatives Squared:* Minimizing the squared torque derivatives which in our case are the controls, is used as a regularization term for the objective function.

$$\phi_{L_6}(t, \boldsymbol{x}(t), \boldsymbol{u}(t), \boldsymbol{p}) = \|\boldsymbol{u}(t)\|_2^2 . \tag{13}$$

*g) Minimize Head Angle:* The objective function

$$\phi_{L_7}(t, \boldsymbol{x}(t), \boldsymbol{u}(t), \boldsymbol{p}) = \|\theta_{head,abs}\|_2^2 \tag{14}$$

is formulated as a criterion for head stabilization as an athlete keeps his head upwards during the constant velocity phase of a sprinting race.

*h) Minimize Angular Momentum:* In upright motions the average total angular momentum about the center of mass should be zero. The following objective function of Lagrange type is a measure of how much the actual angular momentum $\boldsymbol{l}_{CoM}(\boldsymbol{q}(t), \dot{\boldsymbol{q}}(t))$ deviates from zero:

$$\phi_{L_8}(t, \boldsymbol{x}(t), \boldsymbol{u}(t), \boldsymbol{p}) = \|\boldsymbol{l}_{CoM}(\boldsymbol{q}(t), \dot{\boldsymbol{q}}(t))\|_2^2 . \tag{15}$$

*i) Maximize Vertical Ground Reaction Force:* The ground reaction forces are the opposite forces to the ones the sprinter applies to the ground during contact. Hence, the following objective function which is formulated to maximize the vertical ground reaction force, is only evaluated within the contact phases:

$$\phi_{L_9}(t, \boldsymbol{x}(t), \boldsymbol{u}(t), \boldsymbol{p}) = -f^2_{vertical} . \tag{16}$$

*j) Maximize Horizontal Ground Reaction Force:* We now consider the horizontal component of the ground reaction forces which again is only evaluated during contact phases:

$$\phi_{L_{10}}(t, \boldsymbol{x}(t), \boldsymbol{u}(t), \boldsymbol{p}) = -f^2_{horizontal} . \tag{17}$$

Table I summarizes the investigated objective functions which we defined by choosing weightings $\gamma_j$: The criterion which is formulated in the 'Name'-column is the main contribution to the objective functions $\phi_1, \ldots, \phi_{10}$. For some of those criteria it might happen that the optimization does not yield a unique, but a set of solutions. To select one solution, we add a small weighting of the $\phi_{L_6}$- term which additionally serves as a regularization term. The objective functions $\phi_{11}$ $\phi_{12}$ minimize a combination of optimality criteria. The weightings are chosen such that they account for both the importance of the respective criterion for sprinting motions and the different orders of magnitude.

### B. Numerical Solution of the Optimal Control Problem

To solve the multi-phase optimal control problem, we employ the software package MUSCOD-II [2], [12]. For the numerical solution, the control variables are discretized by piecewise linear functions and the state variables are parametrized by the multiple shooting method. To ensure a continuous solution, continuity constraints are imposed at the shooting interval transitions for all state variables. The result of the parametrization is a large non-linear programming problem which is solved by a specially tailored sequential quadratic programming (SQP) method.

## IV. NUMERICAL RESULTS AND DISCUSSION

For each of the objective functions $\phi_1, \ldots, \phi_{11}$, we computed an able-bodied and an amputee sprinting motion. For

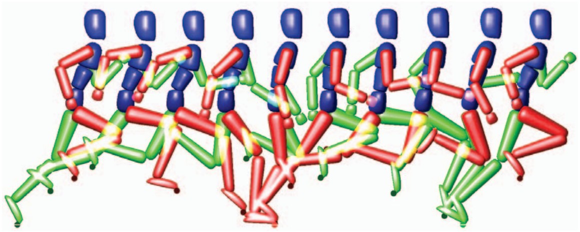

(a) Able-bodied sprinting for *Multiple Objective Criteria I*

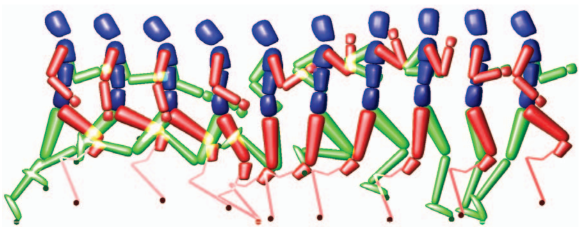

(b) Amputee sprinting for *Max. Step Frequency*

Fig. 4: Visualization of synthesized sprinting motions

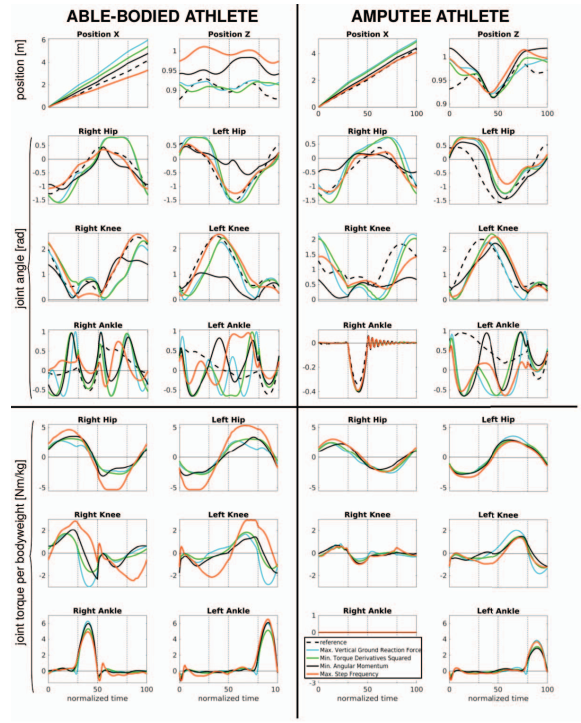


Fig. 5: Comparison of the objective functions *Max. Vertical Ground Reaction Force*, *Min. Torque Derivatives Squares*, *Min. Angular Momentum* and *Max. Step Frequency* for able-bodied and amputee sprinting. The plots show the overall position (top row), the leg joint angles (rows 2–4) and the leg joint torques (last three rows). The dashed line shows the solution of the dynamics reconstruction [11].

each, we show a visual representation of the solutions in Fig. 4. In this section, we analyze the numerical results of the optimal control problem to answer the research questions that we posed in the introduction.

*1) Which optimality criteria are adopted in human sprinting with and without prostheses?*
To evaluate which optimality criteria are a good description of real human sprinting, we compare the obtained motions to motion capture recordings for each of the objective functions $\phi_1, \ldots, \phi_{12}$. Figure 5 shows exemplarily the leg joint angles and torques for five selected objective functions that range from high to low similarity. As reference, we use results of a previous study [11] in which the dynamics of sprinting motions from one able-bodied and one amputee athlete was reconstructed from purely kinematic motion capture. This was achieved by a least squares fit to the data using the identical models as in the present work. From the formulation of position constraints, we can reconstruct the ground reaction forces and joint torques even if they are not measured. As an attempt to identify the most human-like motions, we define a similarity measure

$$d\big(\boldsymbol{q}^S(t)\,, \boldsymbol{q}^M_{,}(t)\, t_f^S, t_f^M\big) = \sum_{j=1}^{4} \left|t_{f,j}^S - t_{f,j}^M\right| \qquad (18)$$
$$+ \frac{1}{m}\sum_{i=1}^{m}\sum_{j=1}^{4}\left(\frac{1}{n_{dof_j}}\left\|\boldsymbol{q}_j^S(i\Delta t) - \boldsymbol{q}_j^M(i\Delta t)\right\|_2\right)\,,$$

which computes the temporal and postural deviations between the synthesized and the reconstructed solution – the smaller the similarity measure the closer the two motions match each other. The postural and temporal similarity calculations are each divided into four groups: the overall position, legs, arms and torso and the flight and contact phases (corresponding to $j = 1, \ldots, 4$). The superscripts $S$ and $M$ denote the synthesized and the motion capture data, respectively. The number of degrees of freedom $n_{dof_j}$ is evaluated per group and $m$ is the number of function evaluations. Figure 6 shows the results of postural and temporal similarities for an evaluation of $m = 1000$.

For the able-bodied athlete, the function *Multiple Objective Criteria I* has the smallest similarity value which corresponds to highest similarity between the synthesized and the reconstructed solutions. This function combines the *Max. Step Frequency*, *Max. Stride Length*, *Min. Torque Derivatives Squared* and *Head Stabilization* functions. In terms of similarity value, it is followed by the functions *Min. Torque Derivatives Squared*, *Max. Step Frequency* and *Min. Angular Momentum*. It seems that the able-bodied athlete whose motion capture data is used as a reference, aims to increase both step frequency and step length. However, the fact that the similarity measure of the function *Max. Stride Length* is about $40\,\%$ bigger than the one of *Max. Step Frequency*, underlines the inverse relation between the two quantities. This suggests that the reference athlete has found his optimal way of sprinting at maximum speed by increasing the step frequency a bit more than the step length. The *Min. Torque Derivatives Squared* function which has a high similarity value as well enforces smooth trajectories. It is notable that the above mentioned functions have best temporal similarity values, but none of them is in the top three functions in terms of postural similarity (those are *Max.*

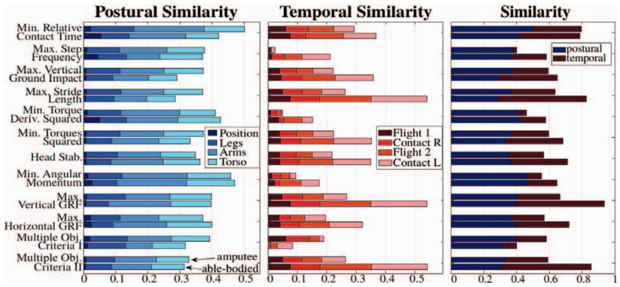


Fig. 6: Postural and temporal similarity of the generated motions and motion capture data for different objective functions. In each case, the lower bar shows the able-bodied and the upper bar the amputee results.

*Stride Length*, *Max. Vertical Ground Impact* and *Multiple Objective Criteria II*).

In the amputee case, we find the smallest similarity value for the function *Max. Step Frequency*, closely followed by *Min.Torque Derivatives Squared* and *Min. Angular Momentum*. Hence, we find similar functions as in the able-bodied case. Again, this is in large parts due to the high temporal similarity. The functions *Multiple Objective Criteria II*, *Head Stabilization*, *Max. Horizontal Ground Reaction Force* and *Max. Stride Length* are the best in terms of postural similarity. It is interesting to note that in the amputee case the *Multiple Objective Criteria I* function does not lead to a high similarity, but both *Max. Step Frequency* and *Max. Stride Length* are good either in terms of temporal or postural similarity. Hence, there should be a combination of those two functions that lead to very realistic motions, but the weighting needs to be different to the able-bodied one.

We now want to compare the able-bodied and amputee similarity measures: The similarity between the synthesized and the reference movements is much better in the amputee case for many of the objective functions. We should keep in mind that we compare the synthesized sprinting motions only to the motion capture recordings of one able-bodied and one amputee athlete. Hence, it might be that these individual athletes found a way of sprinting which is optimal for them, but does not apply to all sprinters. While we know for sure that the amputee athlete competes at world level, for the able-bodied athlete we only know that he is well trained. Nevertheless, a possible explanation would be that there actually is a difference in the optimality criteria for able-bodied and amputee sprinting. As both have small similarity values for the function *Max. Step Frequency* we still can conclude that this is actually a key factor in sprinting. When considering the visualizations of the motions (see video attachment), it is worth mentioning that many of the objective functions produce motions which resemble human sprinting, but are unfeasible in single limbs (e.g. by having unrealistic arm movements). Thus, it might be interesting to impose objective functions more specifically to single groups of limbs as we already did in the *Head Stabilization* function for the head.

In summary, we found optimality criteria that lead to realistic human sprinting motions. Still, we cannot answer the question conclusively, but need to compare the synthesized data to a larger set of motion capture data for sprinting.

*2) Are the joint torques significantly lower in the sprinting solution of the unilateral transtibial amputee?*
To compare the joint torques of the able-bodied and amputee athlete for the different optimality criteria, we compute the maximum absolute torques and the average absolute torques normalized by bodyweight for all objective functions. We show them in Fig. 7 per joint. As powered devices are not allowed in sprinting competitions, the active torque of the amputee athlete's right ankle is $\tau_{\text{right ankle}} = 0$.

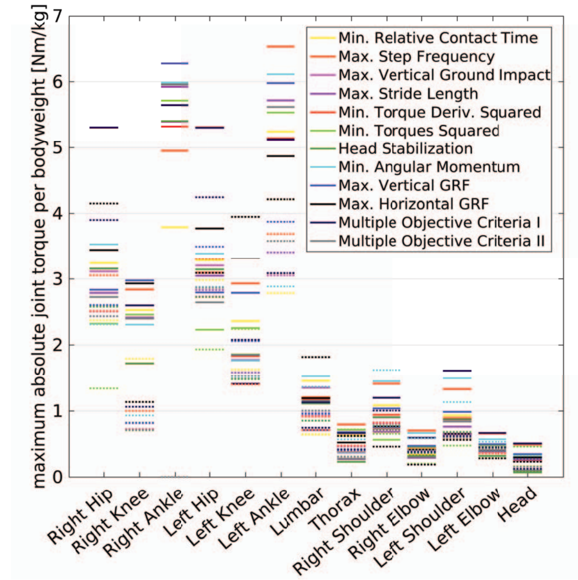


(a) Max. absolute torques per joint for all objective functions

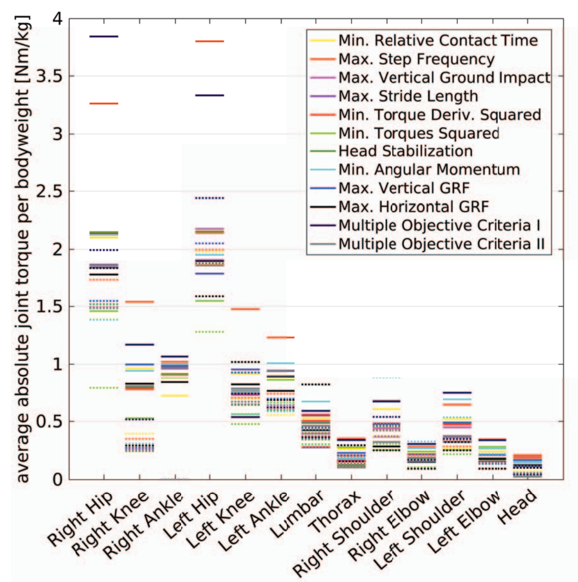


(b) Average absolute torques per joint for all objective functions

Fig. 7: Comparison between the able-bodied (solid lines) and the amputee athlete (dashed lines)

In the joints of the upper body and arms, the maximal and average joint torques are of comparable size for both athletes. We now take a closer look at the joint torques of the legs. They are of comparable size in the unaffected (left) leg for able-bodied and amputee sprinting. For most objective functions, the amputee's joint torques are slightly smaller, for some they are slightly bigger (compare e.g. left hip torques for *Max. Vertical Ground Reaction Force*). In the affected leg, we observe clearly smaller average absolute joint torques for both the hip and the knee joints. If we contrast the right and left leg of the amputee athlete, it is evident that the average joint torques of the affected leg are smaller than the ones of the unaffected leg. For some objective functions, there is also a huge difference between the able-bodied's right and left leg.

We conclude that the passive action of the running-specific prosthesis seems to compensate for some of the work which is actively done in the knee and hip of the able-bodied athlete. As seen before, it is possible to generate sprinting motions by applying a *Min. Torques* objective function, but there are other optimality criteria which lead to more realistic solutions. It is worth mentioning that even for the *Min. Torque* objective function, we cannot find such a clear compensation in unilateral transtibial amputee sprinting as Mombaur [17] found for double transtibial amputee sprinters with a similar objective function. Interestingly, the reconstructed joint torques from the motion capture data of the amputee athlete are significantly higher than the ones we computed with the different objective functions. This leads to new research questions, e.g. why does the amputee athlete not fully exploit the functionality of his prosthesis?

## V. CONCLUSIONS AND FUTURE WORK

We have presented ten optimality criteria which might be applied in human sprinting. For both able-bodied and amputee athletes, we found combinations of criteria which lead to realistic human-like sprinting motions. We further compared the joint torques of the able-bodied and the amputee athlete.

The maximization of velocity is an optimality criteria which probably is of high interest for sprinting motions and which we did not consider in our work. This is due to the fact that for such an optimality criterion, it is necessary to have proper limits for maximum and minimum joint torques. We do not know of any literature that reports such joint limits for elite athletes. However, as stated in the introduction, the sprinting velocity can be approximated as the product of step frequency and step length. We found that both maximizing the step length and maximizing the step frequency yield realistic sprinting motions with high similarity to the motion capture data. This suggests that the athletes whose motion capture recordings were used as reference tried to maximize speed. Nevertheless, in the future we would like to measure joint torque limits in order to formulate a speed maximizing optimality criterion.

As we found considerable differences in the joint torques of the right and the left leg of the amputee athlete, we aim to extend our study to test different optimality criteria for the two legs in order to find out if the legs accomplish different tasks in amputee sprinting.

A deeper understanding of the interaction between human and prosthetic device can be used to improve the design of prostheses.

## ACKNOWLEDGMENT

We want to thank the Simulation and Optimization research group of the IWR at Heidelberg University for giving us the possibility to work with MUSCOD-II.

## REFERENCES

[1] M. Ae, A. Ito, and M. Suzuki, The men's 100 meters. New Studies in Athletics, vol. 7, 1992, pp. 4752.
[2] H.G. Bock, and K.J. Plitt, A multiple shooting algorithm for direct solution of optimal control problems, IFAC, 1984, pp. 242247.
[3] G.-P. Brüggemann, A. Arampatzis, F. Emrich, and W. Potthast, Biomechanics of double transtibial amputee sprinting using dedicated sprinting prostheses, Sports Techn, vol. 1(4-5), 2008, pp. 220227.
[4] K.P. Clark, L.J. Ryan, and P.G. Weyand, A general relationship links gait mechanics and running ground reaction forces, J Exp Biol, vol. 220, 2017, pp. 247258.
[5] M. Felis, and K. Mombaur, Synthesis of Full-Body 3-D Human Gait using Optimal Control Methods, in: IEEE ICRA 2016, 2016, pp. 15601566 .
[6] M. Felis, RBDL: an efficient rigid-body dynamics library using recursive algorithms, Auton Robot, vol. 41(2), 2017, pp. 495511.
[7] H. Geyer 1, A. Seyfarth, and R. Blickhan, Compliant leg behaviour explains basic dynamics of walking and running, Proc R Soc B, vol. 273, 2006, pp. 28612867.
[8] B.K. Higginson, Methods of Running Gait Analysis, Curr Sport Med Rep, vol. 8(3), 2009, pp. 136141.
[9] H. Hobara, Running mechanics in amputee runners using running-specific prostheses, Jpn J Biomechanics Sports Exerc, vol. 17(1), 2013, pp.
[10] H. Hobara, Y. Kobayashi, and M. Mochimaru, Spatiotemporal Variables of Able-bodied and Amputee Sprinters in Mens 100-m Sprint, Int J Sports Med, vol. 36, 2015, pp. 494497.
[11] A.L. Kleesattel, D. Clever, J. Funken, W. Potthast, and K. Mombaur, Modeling and Optimal Control of Able-bodied and Unilateral Amputee Running, ISBS 2017, 2017, pp. 164167.
[12] D.B. Leineweber, I. Bauer, H.G. Bock, and J.P. Schlöder, An Efficient Multiple Shooting Based Reduced SQP Strategy for Large-Scale Dynamic Process Optimization (Parts I and II), Comput Chem Eng, vol. 27(2), 2003, pp. 157174.
[13] P. de Leva, Adjustments to Zatsiorsky-Seluyanov's segment inertia parameter, J Biomech, vol. 29, 1996, pp. 12231230.
[14] R.V. Mann, A kinetic analysis of sprinting, Med Sci Sport Exer, vol. 13(5), 1981, pp. 325328.
[15] R.H. Miller, B.R. Umberger, and G.E. Caldwell, Limitations to maximum sprinting speed imposed by muscle mechanical properties, J Biomech, vol. 45, 2012, pp. 10921097.
[16] A.A. Mero, P.V. Komi, and R. Gregor, Biomechanics of Sprint Running: A Review, Sports Med, vol. 13(6), 1992, pp. 376392.
[17] K. Mombaur, A Mathematical Study of Sprinting on Artificial Legs, in: HPSC 2012, 2014, pp. 157168.
[18] A.I.T. Salo, I.N. Bezodis, A.M. Batterham, and D.G. Kerwin, Elite Sprinting: Are Athletes Individually Step-Frequency of Step-Length Reliant?, Med Sci Sport Exer, vol. 43(6), 2011, pp. 10551062.
[19] A.G. Schache, T.W. Dorn, P.D. Blanch, N.A.T. Brown, and M.G. Pandy, Mechanics of the Human Hamstring Muscles during Sprinting, Med Sci Sport Exer, vol. 44(4), 2012, pp. 647658.
[20] G. Schultz, and K. Mombaur, Modeling and Optimal Control of Human-Like Running, Trans Mechatron, vol. 5(5), 2010, pp. 783792.
[21] P.G. Weyand, D.B. Sternlight, M.J. Bellizzi, and S. Wright, Faster top running speeds are achieved with greater ground forces not more rapid leg movements, J Appl Physiol, vol. 89, 2000, pp. 19911999.
[22] P.G. Weyand, M.W. Bundle, C.P. McGowan, A. Grabowski, M.B. Brown, R. Kram, and H. Herr, The fastest runner on artificial legs: different limbs, similar function?, J Appl Physiol, vol. 107(3), 2009, pp. 903911.